

Status Report on the Development of a Thermodynamic Database for Use with Metallic Fuel Design

Chao Jiang, Robert D Mariani

September 2018



The INL is a U.S. Department of Energy National Laboratory
operated by Battelle Energy Alliance

Status Report on the Development of a Thermodynamic Database for Use with Metallic Fuel Design

Chao Jiang, Robert D Mariani

September 2018

**Idaho National Laboratory
Idaho Falls, Idaho 83415**

<http://www.inl.gov>

**Prepared for the
U.S. Department of Energy**

**Under DOE Idaho Operations Office
Contract DE-AC07-05ID14517**

***Status report on the
development of a
thermodynamic database for
use with metallic fuel design***

**Nuclear Technology
Research and Development**

***Prepared for
U.S. Department of Energy
Advanced Fuels Campaign
Chao Jiang, Robert Mariani
INL National Laboratory
August 2018
NTRD-FUEL-2018-000087***



DISCLAIMER

This information was prepared as an account of work sponsored by an agency of the U.S. Government. Neither the U.S. Government nor any agency thereof, nor any of their employees, makes any warranty, expressed or implied, or assumes any legal liability or responsibility for the accuracy, completeness, or usefulness, of any information, apparatus, product, or process disclosed, or represents that its use would not infringe privately owned rights. References herein to any specific commercial product, process, or service by trade name, trade mark, manufacturer, or otherwise, does not necessarily constitute or imply its endorsement, recommendation, or favoring by the U.S. Government or any agency thereof. The views and opinions of authors expressed herein do not necessarily state or reflect those of the U.S. Government or any agency thereof.

SUMMARY

The scope of this FY18 milestone involves the development of a high fidelity thermodynamic database for the U-Mo-Ti-Zr system to support the accelerated design of new pseudo-binary U- x M metallic fuel, where M is a ternary metallic additive composed of Mo, Ti and Zr and x is the additive amount. Based on the previous assessment of the Mo-Ti-Zr ternary system performed in FY17, a complete set of thermodynamic model parameters describing the U-Mo-Ti-Zr quaternary system over the entire composition and temperature range have been developed in this work using the CALPHAD (CALculation of PHase Diagrams) approach with inputs from both experimental measurements and density functional theory (DFT) total energy calculations. The two ternary intermetallic compounds, the delta phase in the U-Ti-Zr system and the cubic C15 Laves phase in the Mo-Ti-Zr system, are modeled using physically-based two-sublattice compound energy formalism. The liquid, bcc and hcp phases are described using the random solution model. Using the present database, the melting temperatures and bcc onset temperatures of U- x M metallic fuels are predicted as a function of both additive composition and amount. An optimal metallic additive composition has been identified in this work.

INTENTIONALLY BLANK

CONTENTS

SUMMARY	iii
ACRONYMS	vii
1. INTRODUCTION.....	1
2. COMPUTATIONAL METHOD	1
2.1 The CALPHAD Approach.....	1
2.2 Density Functional Theory Calculations	3
3. RESULTS	5
3.1 Mo-Ti-Zr.....	5
3.2 U-Ti-Zr	5
3.3 U-Mo-Zr	5
3.4 U-Mo-Ti.....	7
3.5 Computational Screening of U-Mo-Ti-Zr Fuel Alloys.....	7
4. CONCLUSION	9
5. REFERENCES.....	9

FIGURES

Figure 1. (a) Direct comparisons between the mixing energies of 69 ordered Laves structures predicted by DFT calculations and cluster expansion. The solid line represents perfect agreement between the two methods. (b) Monte Carlo simulated mixing energies of disordered (Mo,Ti) ₂ Zr Laves phase at 873 K.	3
Figure 2. Model predicted Mo-Ti-Zr isothermal sections at (a) 600°C and (b) 750°C in comparison with experimental measurements from Prokoshkin and Zakharova [3].	5
Figure 3. Model predicted U-Ti-Zr isothermal sections at (a) 700°C and (b) 800°C in comparison with experimental measurements from Howlett [7].	6
Figure 4. U-Mo-Zr isothermal section at 625°C from (a) experiments [8] and (b) present modeling.	6
Figure 5. U-Mo-Zr isothermal section at 700°C from (a) experiments [8] and (b) present modeling.	7
Figure 6. Model predicted U-Mo-Ti isothermal sections at (a) 600°C and (b) 700°C.	7
Figure 7. Model predicted equilibrium phase fractions for U ₉₀ Mo _{2.5} Ti _{2.5} Zr ₅ vs. temperature.	8
Figure 8. Prediction of the bcc onset temperatures and melting temperatures of U-xM pseudo binary fuels where M is a Mo-Ti-Zr alloy and x=0, 0.05, 0.10, and 0.15.	8

TABLES

Table 1. Thermodynamic parameters for the U-Mo-Ti-Zr quaternary system.	4
--	---

INTENTIONALLY BLANK

ACRONYMS

CALPHAD	CALculation of PHAse Diagrams
DFT	Density Functional Theory
GGA	generalized gradient approximation
PBE	Perdew-Burke-Ernzerhof
SGTE	Scientific Group Thermodata Europe
VASP	Vienna ab initio simulation package

INTENTIONALLY BLANK

STATUS REPORT ON THE DEVELOPMENT OF A THERMODYNAMIC DATABASE FOR USE WITH METALLIC FUEL DESIGN

1. INTRODUCTION

Alloying uranium (U) with metallic additives is a viable way to produce nuclear fuels with increased burnup (fuel utilization) and improved chemical, thermal, and mechanical properties. For example, compared with pure U, a pseudo-binary U- x M fuel mixture may simultaneously exhibit higher melting temperature (for increased safety margin) and enhanced phase stability of body-centered cubic (bcc) γ -U against phase transformation to α -U at lower temperatures [1]. Here, M is a metallic additive that can be an elemental metal or an alloy of metals, and x is its relative amount in the fuel. For candidates of M, while pure molybdenum (Mo) is a strong γ -U stabilizer and can significantly depress the bcc-phase onset temperature, its addition does not lead to large increase in melting temperature compared to pure U, as indicated by the almost flat solidus line in the binary U-Mo phase diagram. Conversely, while both zirconium (Zr) and titanium (Ti) can strongly raise the melting point of γ -U, the bcc onset temperature is not much decreased by their addition. By using a ternary Mo-Ti-Zr alloy as metallic additive, it is possible to design U-Mo-Zr-Ti alloys that can take advantage of the bcc phase stabilization offered by Mo while not compromising the melting temperature via the addition of Zr and Ti.

While the optimum composition of the Mo-Ti-Zr metallic additive and its amount can be identified by performing a large number of experimental measurements, the process can be both time-consuming and costly. To expedite the fuel alloy design process, a high fidelity thermodynamic database describing the U-Mo-Ti-Zr quaternary system over the entire composition and temperature range has been developed in this work using the CALPHAD approach with inputs from both experimental measurements published in the literature and highly predictive DFT energetics. Due to the scarcity of experimental data for the U-Mo-Ti-Zr system, the incorporation of DFT data is of crucial importance for guaranteeing the quality of the database. Using the present database, the melting temperature (i.e., the solidus temperature) and bcc onset temperature of U- x M metallic fuel are predicted as a function of both additive composition and amount. Such results can be directly used to guide the design of advanced metallic fuel alloys.

2. COMPUTATIONAL METHOD

2.1 The CALPHAD Approach

CALPHAD (CALculation of PHase Diagrams) is a self-consistent approach that links the underlying thermodynamics and phase equilibria of multi-component systems using both physically-based and phenomenological models that describe the Gibbs free energy of each individual phase in a system as a function of temperature, composition, and possibly also pressure. The key strength of the CALPHAD approach is that it allows the phase diagrams and properties of a high-order multi-component alloy to be predicted based on extrapolation from the information of its unary, binary and ternary sub-systems. For example, a quaternary A-B-C-D phase diagram can be predicted using only the free energies of phases in its binary (A-B, A-C, A-D, B-C, B-D, C-D) and ternary (A-B-C, A-B-D, B-C-D) subsystems. Such predictions are highly valuable when experimental data are scarce, which is the case for the U-Mo-Ti-Zr system.

The liquid, bcc and hcp solution phases are described using the random solution model, which assumes completely random mixing of alloying elements on a single parent lattice, neglecting the effects of short-range ordering. Their free energies can be written using Equation 1, where Φ =liquid, bcc or hcp. x_i represents the mole fraction of element i (U, Mo, Ti, Zr). G_i^Φ is the Gibbs energy of pure element i in structure Φ , which can be taken from the Scientific Group Thermodata Europe (SGTE) pure element

database, with the reference state being the enthalpies of the pure elements in their stable states at 298.15K, commonly referred to as Standard Element Reference. $L_{i,j}$ represents the binary interaction parameter between elements i and j , which describes the deviation of real i - j alloy from the ideal solution behavior. Similarly, $L_{i,j,k}$ is the ternary interaction parameter between elements i , j and k .

As shown in Equation 2, the composition-dependence of the binary interaction parameters can be written in the form of a Redlich-Kister polynomial. $L_{i,j}^k$ is the k -th interaction parameter between elements i and j and can be temperature-dependent in the form $L_{i,j}^k = a + bT$, where the coefficients a and b have the physical meaning as the enthalpy and entropy of mixing, respectively.

In view of the large solubility of Ti in the cubic Mo_2Zr Laves phase in the Mo-Ti-Zr ternary system [3], the Laves phase is modeled using a $(\text{Mo,Ti})_2(\text{Zr})_1$ two-sublattice model and its free energy is shown in Equation 3, where y'_{Mo} and y'_{Ti} denote the site fraction of Mo and Ti in the first sublattice, respectively. $G_{\text{Mo}_2\text{Zr}}$ and $G_{\text{Ti}_2\text{Zr}}$ are the Gibbs free energies of the end-member Mo_2Zr and Ti_2Zr Laves phases.

Since delta- U_2Ti and delta- UZr_2 compounds have the same BiIn_2 -type crystal structure, they are modeled as the same phase using a $(\text{U,Zr})_2(\text{Ti,Zr})_1$ two-sublattice model. Equation 4 shows the Gibbs free energy of the delta phase. Here, y'_U and y'_{Zr} denote the site fraction of U and Zr in the first sublattice, respectively. y''_{Ti} and y''_{Zr} denote the site fraction of Ti and Zr in the second sublattice, respectively.

Finally, intermetallic compound U_2Mo with negligible homogeneity ranges is modeled as a line compound with fixed composition.

Equation 1. Gibbs free energy of U-Mo-Ti-Zr random solution phase

$$G_m^\Phi = x_U G_U^\Phi + x_{\text{Mo}} G_{\text{Mo}}^\Phi + x_{\text{Ti}} G_{\text{Ti}}^\Phi + x_{\text{Zr}} G_{\text{Zr}}^\Phi + RT(x_U \ln(x_U) + x_{\text{Mo}} \ln(x_{\text{Mo}}) + x_{\text{Ti}} \ln(x_{\text{Ti}}) + x_{\text{Zr}} \ln(x_{\text{Zr}})) + x_U x_{\text{Mo}} L_{\text{Mo},U} + x_U x_{\text{Ti}} L_{\text{Ti},U} + x_U x_{\text{Zr}} L_{U,\text{Zr}} + x_{\text{Mo}} x_{\text{Ti}} L_{\text{Mo},\text{Ti}} + x_{\text{Mo}} x_{\text{Zr}} L_{\text{Mo},\text{Zr}} + x_{\text{Ti}} x_{\text{Zr}} L_{\text{Ti},\text{Zr}} + x_U x_{\text{Ti}} x_{\text{Zr}} L_{\text{Ti},U,\text{Zr}} \quad (1)$$

Equation 2. Composition-dependent interaction parameters between elements i and j

$$L_{i,j} = \sum_{k=0}^n L_{i,j}^k (x_i - x_j)^k \quad (2)$$

Equation 3. Gibbs free energy of the Laves phase in Mo-Ti-Zr system

$$G_m = y'_{\text{Mo}} G_{\text{Mo}_2\text{Zr}} + y'_{\text{Ti}} G_{\text{Ti}_2\text{Zr}} + RT(y'_{\text{Mo}} \ln(y'_{\text{Mo}}) + y'_{\text{Ti}} \ln(y'_{\text{Ti}})) + y'_{\text{Mo}} y'_{\text{Ti}} (L_{\text{Mo,Ti:Zr}}^0 + L_{\text{Mo,Ti:Zr}}^1 (y'_{\text{Mo}} - y'_{\text{Ti}})) \quad (3)$$

Equation 4. Gibbs free energy of the delta phase in U-Ti-Zr system

$$G_m = y'_U y''_{\text{Ti}} G_{\text{U}_2\text{Ti}} + y'_U y''_{\text{Zr}} G_{\text{U}_2\text{Zr}} + y'_{\text{Zr}} y''_{\text{Ti}} G_{\text{Zr}_2\text{Ti}} + y'_{\text{Zr}} y''_{\text{Zr}} G_{\text{Zr}_2\text{Zr}} + 2RT(y'_U \ln(y'_U) + y'_{\text{Zr}} \ln(y'_{\text{Zr}})) + RT(y''_{\text{Ti}} \ln(y''_{\text{Ti}}) + y''_{\text{Zr}} \ln(y''_{\text{Zr}})) + y'_U y'_{\text{Zr}} y''_{\text{Zr}} (L_{U,\text{Zr:Zr}}^0 + L_{U,\text{Zr:Zr}}^1 (y'_U - y'_{\text{Zr}})) + y'_U y'_{\text{Zr}} y''_{\text{Ti}} L_{U,\text{Zr:Ti}} \quad (4)$$

In this work, the unknown model parameters are obtained by fitting to both DFT energies and experimental phase equilibrium data such as liquidus, solidus, and invariant reaction temperatures. The optimization of model parameters is performed using the Parrot module in Thermo-Calc, which works by minimizing the weighted sum of differences between calculated and experimentally measured values using nonlinear least-square regression. Different types of experimental data, e.g., thermochemical and phase equilibrium ones, are optimized simultaneously. The weight for each piece of experimental data is chosen according to its experimental uncertainty and relative importance. A final global optimization is performed, in which all unknown model parameters are optimized simultaneously, with all experimental

data included. This ensures the best possible agreement between model calculations and experimental data. Parameters for binary U-Mo, U-Ti and U-Zr systems are not optimized in this work. These data are collected from previous studies [4,5]. The final optimized model parameters are given in Table 1.

2.2 Density Functional Theory Calculations

DFT calculations are performed using the projector augmented wave method within the generalized gradient approximation (GGA), as implemented in the Vienna ab initio simulation package (VASP). For the GGA exchange-correlation functional, we employ the Perdew-Burke-Ernzerhof (PBE) parameterization. The semi-core $3p$ electrons of Ti, the semi-core $4p$ electrons of Mo, and both the semi-core $4s$ and $4p$ electrons of Zr are explicitly treated as valence electrons. The plane wave cutoff energy is set at 350 eV. The k -point meshes for Brillouin zone sampling are constructed using the Monkhorst–Pack scheme, and the total number of k -points times the total number of atoms per unit cell is at least 5000 for all structures. Convergence tests show that the chosen cutoff energy and k -point density are sufficient to guarantee high numerical accuracy. By computing the quantum-mechanical forces and stress tensor, the unit cell volume and shape as well as all internal atomic positions of all structures are fully relaxed using a conjugate-gradient scheme.

In FY18, a new physically-based $(\text{Mo,Ti})_2(\text{Zr})_1$ two-sublattice model has been adopted to describe the Laves phase in the Mo-Ti-Zr system. To parameterize this new model, we have predicted the mixing energies between Mo and Ti in the first sublattice of the Laves phases using a combination of DFT calculations, a cluster expansion technique [6], and Monte-Carlo simulations. Using DFT calculated total energies of 69 ordered Laves structures, we have parameterized a cluster expansion that is capable of predicting the energetics of any distribution of Mo and Ti in the first sublattice of the Laves phase. As shown in Figure 1, the cluster expansion can accurately reproduce the mixing energies predicted by DFT. Importantly, the negative mixing energies indicate that it is thermodynamically favorable to substitute Ti for Mo in the Mo_2Zr Laves phase, which is in agreement with the experimentally observed large solubility of Ti in this binary compound [3]. The mixing energy data shown in Figure 1 are critical for the development of a new thermodynamic description of the Mo-Ti-Zr ternary system in this work.

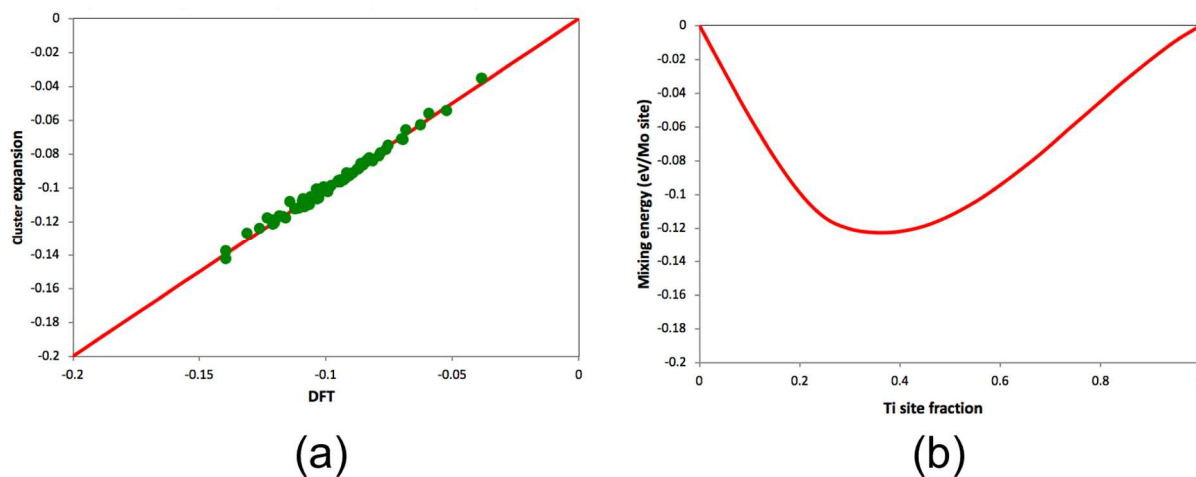


Figure 1 (a) Direct comparisons between the mixing energies of 69 ordered Laves structures predicted by DFT calculations and cluster expansion. The solid line represents perfect agreement between the two methods. (b) Monte Carlo simulated mixing energies of disordered $(\text{Mo,Ti})_2\text{Zr}$ Laves phase at 873 K.

Table 1. Thermodynamic parameters for the U-Mo-Ti-Zr quaternary system.

Phase	Sublattice Model	Parameter	Reference
Liquid	(U, Mo, Ti, Zr) ₁	$L_{Mo,Ti}^0 = -35004-2.013*T$	This work
		$L_{Mo,Ti}^1 = 10517-12.519*T$	This work
		$L_{Mo,Zr}^0 = -14321+4.693*T$	This work
		$L_{Mo,Zr}^1 = -3701+3.648*T$	This work
		$L_{Ti,Zr}^0 = 8902-11.873*T$	This work
		$L_{U,Zr}^0 = 33465.2-14.55*T$	[4]
		$L_{U,Zr}^1 = 19809.4-18.07*T$	[4]
		$L_{Ti,U}^0 = -4174+16.13*T$	[5]
		$L_{Mo,U}^0 = 66600-48.5*T$	[5]
		$L_{Mo,U}^1 = -17400+35.6*T$	[5]
		$L_{Mo,U}^2 = 81300-55*T$	[5]
Bcc	(U, Mo, Ti, Zr) ₁	$L_{Mo,Ti}^0 = -44366+4.194*T$	This work
		$L_{Mo,Ti}^1 = -26453$	This work
		$L_{Mo,Ti}^2 = -9358$	This work
		$L_{Mo,Zr}^0 = 11911+7.969*T$	This work
		$L_{Mo,Zr}^1 = 8158$	This work
		$L_{Ti,Zr}^0 = 10798-9.124*T$	This work
		$L_{U,Zr}^0 = 23296.9-8.97*T$	[4]
		$L_{U,Zr}^1 = 21149.0-16.93*T$	[4]
		$L_{U,Zr}^2 = 2841.6$	[4]
		$L_{Ti,U}^0 = -18000+23.32*T$	[5]
		$L_{Mo,U}^0 = 26180-9.2*T$	[5]
		$L_{Mo,U}^1 = 28370+2.2*T$	[5]
		$L_{Mo,U}^2 = 47200-25*T$	[5]
		$L_{Ti,U,Zr} = -20000$	This work
		$L_{Mo,Ti}^0 = 43508$	This work
Hcp	(U, Mo, Ti, Zr) ₁	$L_{Mo,Zr}^0 = 111808$	This work
		$L_{Ti,Zr}^0 = 20605-13.967*T$	This work
		$L_{U,Zr}^0 = 24184.4$	[4]
		$L_{Ti,U}^0 = 17240$	[5]
		$L_{Ti,U,Zr} = -20000$	This work
Laves	(Mo, Ti) ₂ (Zr) ₁	$G_{Mo_2Zr} - 2G_{Mo}^{bcc} - G_{Zr}^{hcp} = -39203+9.472*T$	This work
		$G_{Ti_2Zr} - 2G_{Ti}^{hcp} - G_{Zr}^{hcp} = 57935$	This work
		$L_{Mo,Ti,Zr}^0 = -88402$	This work
		$L_{Mo,Ti,Zr}^1 = -48619$	This work
U ₂ Mo	(U) ₂ (Mo) ₁	$G_{U_2Mo} - 2G_U^{\alpha-U} - G_{Mo}^{bcc} = -20000+20*T$	[5]
Delta	(U, Zr) ₂ (Ti, Zr) ₁	$G_{U_2Ti} - 2G_U^{\alpha-U} - G_{Ti}^{hcp} = -59000+37.92*T$	[5]
		$G_{U_2Zr} - 2G_U^{\alpha-U} - G_{Zr}^{hcp} = 1764.57+8.304*T$	[4]
		$G_{Zr_2Zr} - 3G_{Zr}^{hcp} = 1582.5$	[4]
		$G_{Zr_2Ti} - 2G_{Zr}^{hcp} - G_{Ti}^{hcp} = 19992$	This work
		$L_{U,Zr,Zr}^0 = -6629.3+20.22*T$	[4]
		$L_{U,Zr,Zr}^1 = 710.1-17.62*T$	[4]
		$L_{U,Zr,Ti}^0 = 195699$	This work

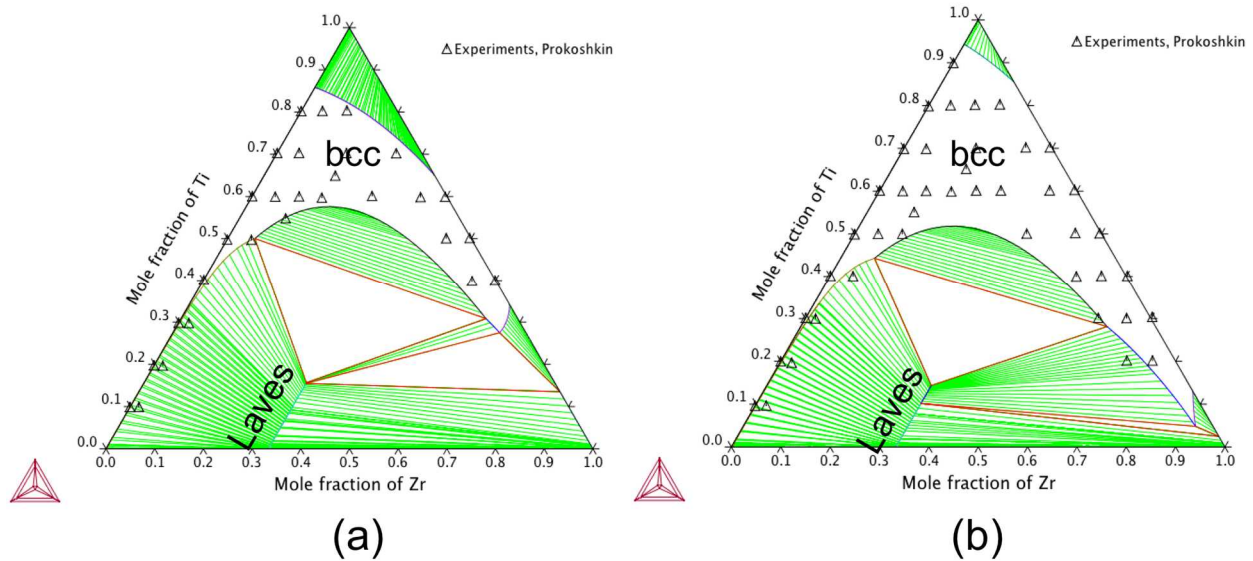


Figure 2. Model predicted Mo-Ti-Zr isothermal sections at (a) 600°C and (b) 750°C in comparison with experimental measurements from Prokoshkin and Zakharova [3].

3. RESULTS

3.1 Mo-Ti-Zr

Based on the previous assessment of the Mo-Ti-Zr ternary system performed in FY17, a new thermodynamic description of the Mo-Ti-Zr system has been developed in FY18 using the newly calculated DFT data for the Laves phase as shown in Figure 1. The most significant improvement is the adoption of a new $(\text{Mo,Ti})_2(\text{Zr})_1$ two-sublattice model for the Laves phase. Figure 2 shows the isothermal sections of the Mo-Ti-Zr ternary system at 600°C and 750°C calculated using the new description. The green lines are tie-lines and the red triangles indicate three-phase equilibrium. At both temperatures, the calculated bcc single-phase region is in excellent agreement with the experimental data from Prokoshkin and Zakharova [3]. For the Mo-Ti-Zr system, no ternary interaction parameter needs to be used.

3.2 U-Ti-Zr

Phase diagrams for U-Ti-Zr system has been experimentally measured by Howlett [7] using x-ray diffraction and optical microscopy techniques. Since both $\delta\text{-U}_2\text{Ti}$ and $\delta\text{-UZr}_2$ compounds in this system have the BiIn_2 -type crystal structure, they are treated as one phase by a $(\text{U,Zr})_2(\text{Ti,Zr})_1$ two-sublattice model. For this system, a ternary interaction parameter ($L_{\text{Ti,U,Zr}} = -20000 \text{ J/mol}$) for the bcc phase needs to be introduced in order to reproduce the experiments from Howlett [7]. As shown in Figure 3, the calculated U-Ti-Zr phase diagram is in overall good agreement with experimental data. At 800°C, the maximum solubility of Zr in U_2Ti is predicted to be 0.017, which agrees with the experimental value (0.02 [7]). At a lower temperature of 700°C, the solubility of Zr in U_2Ti is predicted to increase to 0.048. Again, the predicted value is in agreement with the experimental value of 0.04 from Howlett [7].

3.3 U-Mo-Zr

By combining the thermodynamic parameters for Mo-Zr (from this work), U-Mo [5] and U-Zr [4] binary systems, the isothermal sections of U-Mo-Zr ternary system at 625°C and 700°C are calculated and compared with the experimental phase diagram from Ivanov and Bagrov [8]. As shown in Figure 4 and Figure 5, the calculated phase diagrams are in good agreement with experiments without the need to introduce any ternary interaction parameters. Experimentally, U shows no solubility in the Mo_2Zr Laves

phase, which justifies the neglect of U in the $(\text{Mo,Ti})_2(\text{Zr})_1$ sub-lattice model for the Laves phase. Interestingly, experimental phase diagram indicates the existence of a ternary $\text{U}_6\text{Zr}_3\text{Mo}$ compound, which is not considered in this work due to the lack of crystal structure information for this phase. Future experimental exploration of this ternary phase will be of interest.

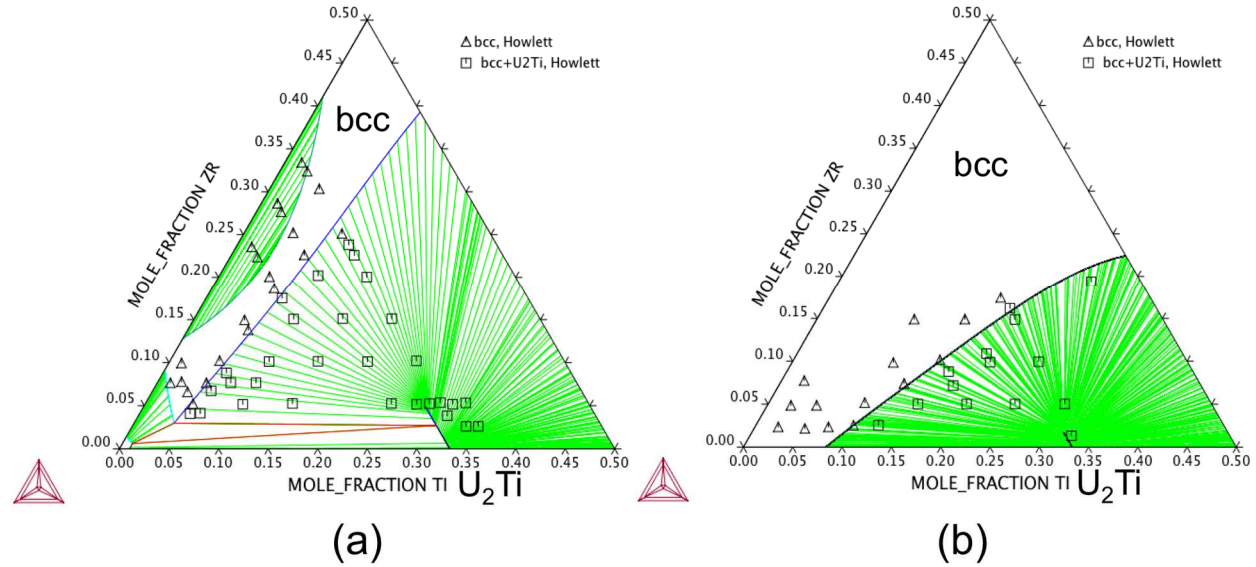


Figure 3. Model predicted U-Ti-Zr isothermal sections at (a) 700°C and (b) 800°C in comparison with experimental measurements from Howlett [7].

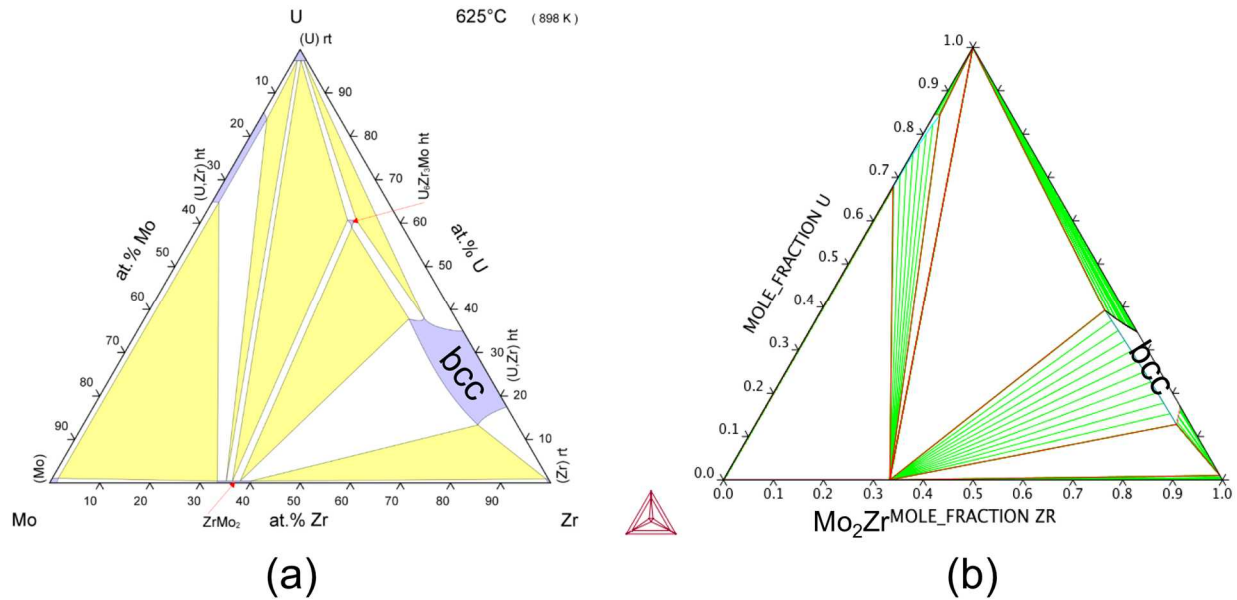


Figure 4. U-Mo-Zr isothermal section at 625°C from (a) experiments [8] and (b) present modeling.

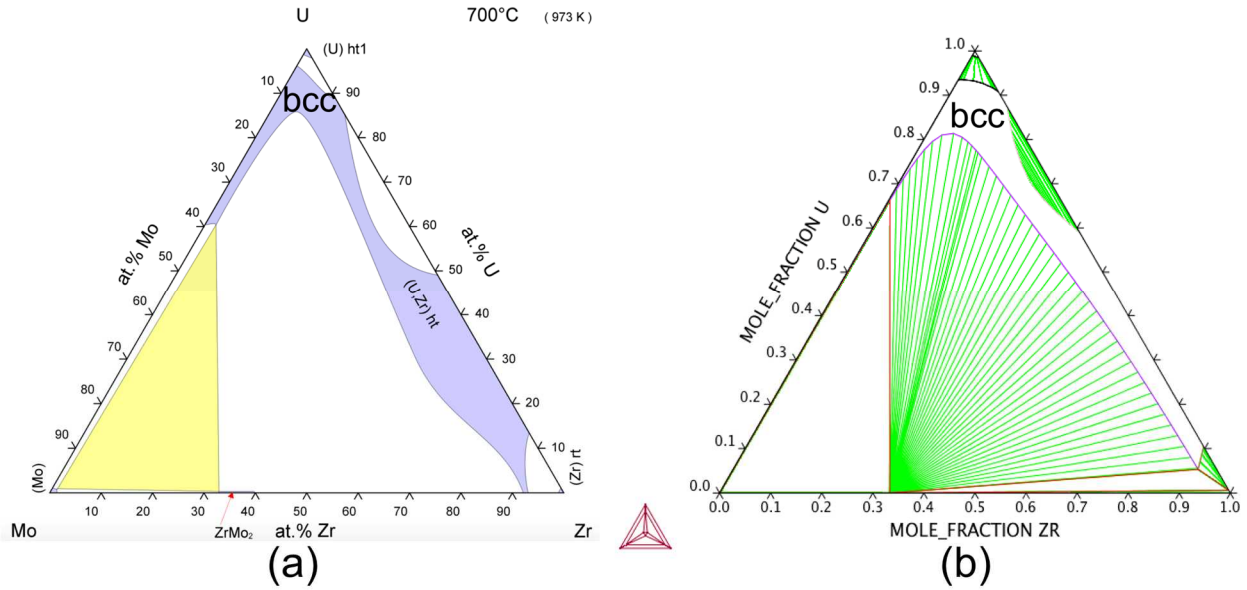


Figure 5. U-Mo-Zr isothermal section at 700°C from (a) experiments [8] and (b) present modeling.

3.4 U-Mo-Ti

No experimental measurement of the U-Mo-Ti system is available in the literature. Its isothermal sections at 600°C and 700°C are calculated in this work and the results are shown in Figure 6.

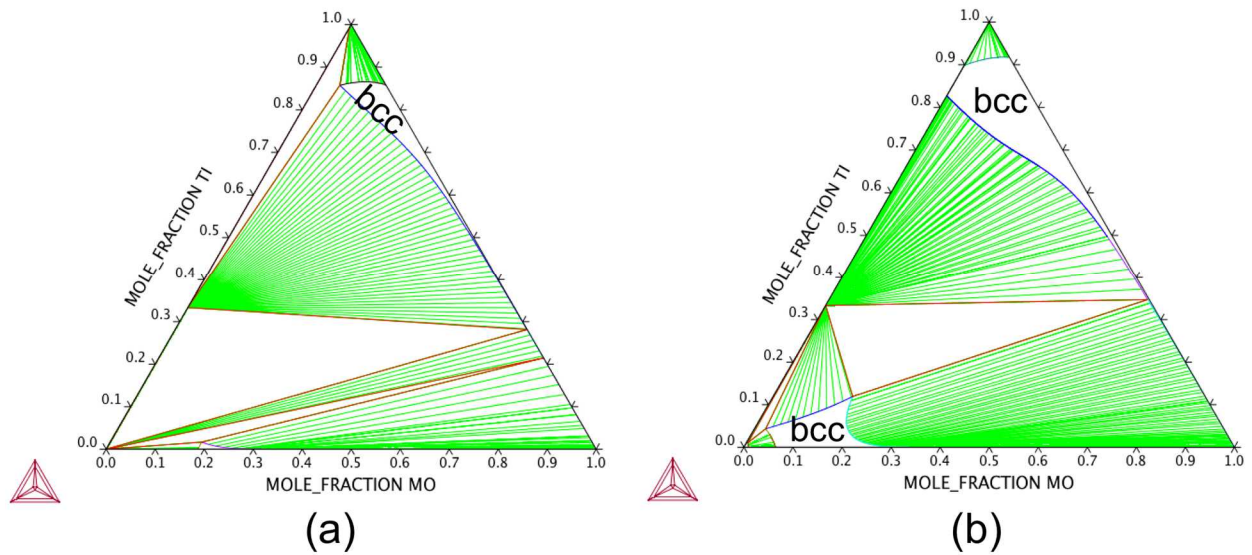


Figure 6. Model predicted U-Mo-Ti isothermal sections at (a) 600°C and (b) 700°C.

3.5 Computational Screening of U-Mo-Ti-Zr Fuel Alloys

Using the present thermodynamic database, one can perform high-throughput computational screening of a large number of U-Mo-Ti-Zr fuel alloys and suggest promising fuel alloy compositions for experimental fabrication and in-reactor performance testing. Figure 7 shows an example virtual heat treatment of a $U_{90}Mo_{2.5}Ti_{2.5}Zr_5$ (at.%) alloy, in which the equilibrium phase fractions are plotted as a function of temperature. The bcc decomposition (or onset) temperature, defined as the lowest temperature for a

single-phase bcc microstructure to be thermodynamically stable, is 953 K for $\text{U}_{90}\text{Mo}_{2.5}\text{Ti}_{2.5}\text{Zr}_5$, which is much lower than that for pure U (1049 K). The solidus temperature for $\text{U}_{90}\text{Mo}_{2.5}\text{Ti}_{2.5}\text{Zr}_5$, which indicates the initiation of melting, is 1436 K. For comparison, the melting temperature of pure U is 1408 K. Figure 8 further shows the calculation results for a large number of U-Mo-Ti-Zr alloys with different additive compositions and amounts ($x=0.05, 0.10, 0.15$). Overall, $\text{Mo}_1\text{Ti}_1\text{Zr}_2$ appears to be one optimal additive composition as its addition to U can significantly stabilize the bcc structure against phase separation and at the same time considerably increase its melting temperature.

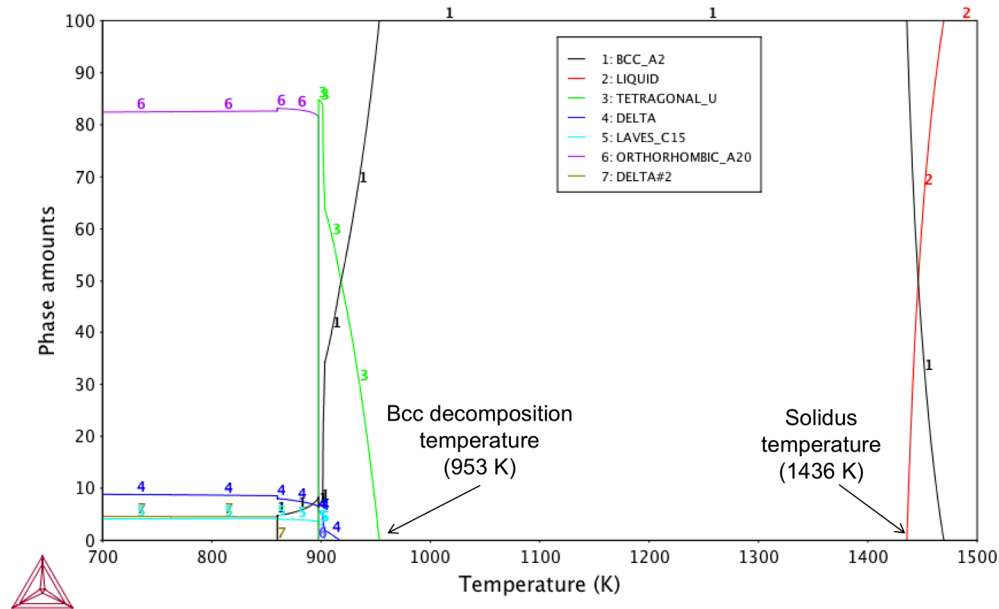


Figure 7. Model predicted equilibrium phase fractions for $\text{U}_{90}\text{Mo}_{2.5}\text{Ti}_{2.5}\text{Zr}_5$ vs. temperature.

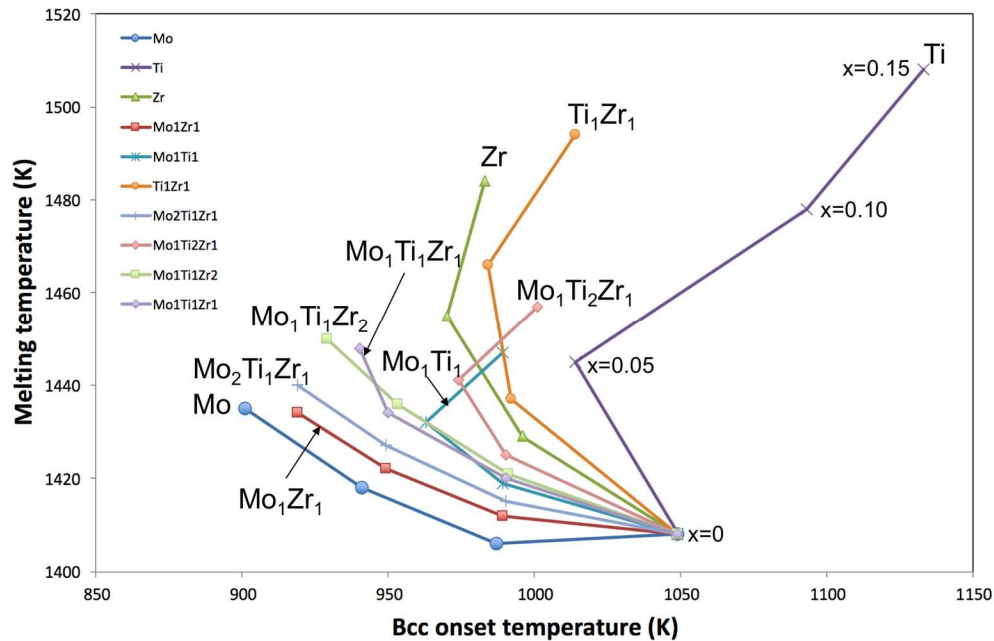


Figure 8. Prediction of the bcc onset temperatures and melting temperatures of U-xM pseudo binary fuels where M is a Mo-Ti-Zr alloy and $x=0, 0.05, 0.10$, and 0.15 .

4. CONCLUSION

During FY18, a high fidelity thermodynamic database for the U-Mo-Ti-Zr quaternary system has been developed using the CALPHAD approach to assist the design of new pseudo-binary U- x M fuel alloy, where M is a bcc Mo-Ti-Zr alloy and x is its amount. The calculated phase diagrams for Mo-Ti-Zr, U-Ti-Zr and U-Mo-Zr ternary systems are all in good agreement with existing experimental data. Extensive DFT calculations have been performed to overcome the scarcity of thermodynamic measurements for these alloys, which is presumably due to experimental difficulties associated with the radioactivity of U, the high melting point of Mo, and the high reactivity of Zr with oxygen at high temperatures. The present thermodynamic database has been employed to predict the melting temperatures and bcc decomposition temperatures of a large number of U-Mo-Ti-Zr fuel alloy compositions, and the results can be valuable for the design of advanced metallic fuels for next-generation nuclear reactors. In future studies, incorporation of other bcc stabilizers such as V, Nb, Ta and W into the database would be of great interest. Since Pd is known to be beneficial in mitigating fuel-cladding chemical interactions, its addition to the database will also be useful.

5. REFERENCES

- [1] R.D. Mariani, D.L. Porter, S.L. Hayes and J.R. Kennedy. Metallic fuels: The EBR-II legacy and recent advances. *Procedia Chemistry*, 7:513-520, 2012.
- [2] M. Hillert. The compound energy formalism. *Journal of Alloys and Compounds*, 320: 161-176, 2001.
- [3] D.A. Prokoshkin and M.I. Zakharova. Isothermal cross sections at 600 and 750C of the phase diagram of the system molybdenum-titanium-zirconium. *Inorg. Mat.*, 3:70-75, 1967.
- [4] W. Xiong, W. Xie, C. Shen and D. Morgan. Thermodynamic modeling of the U-Zr system - A revisit. *Journal of Nuclear Materials*, 443:331-341, 2013.
- [5] A. Berche, N. Dupin, C. Guéneau, C. Rado, B. Sundman and J.C. Dumas. Calphad thermodynamic description of some binary systems involving U. *Journal of Nuclear Materials*, 411:131-143, 2011.
- [6] C. Jiang. Vacancy ordering in Co_3AlC_x alloys. *Physical Review B*, 78:064206, 2008.
- [7] B.W. Howlett. The alloy system uranium-titanium-zirconium. *Journal of Nuclear Materials*, 3:289-299, 1959.
- [8] O.S. Ivanov and G.N. Bagrov. Isothermal cross sections of the triple system uranium-molybdenum-zirconium at 1000°C-625°C. *Struct. Alloys Certain Systems Cont. Uranium Thorium*, 131-153, 1963.